Porphyromonas gingivalis infection induces synaptic failure via increased IL-1β production in leptomeningeal cells

黄, 婉怡

出版情報：Kyushu University, 2021, 博士（歯学）, 課程博士
バージョン：
権利関係：

Porphyromonas gingivalis infection induces synaptic failure via increased IL-1β production in leptomeningeal cells

Wanyi Huang[a], Fan Zeng[a], Yebo Gu[b], Muzhou Jiang[a], Xinwen Zhang[c], Xu Yan[d], Tomoko Kadowaki[e], Shinsuke Mizutani[f,g], Haruhiko Kashiwazaki[f], Junjun Ni[h]*and Zhou Wu[a,g]*

[a]Department of Aging Science and Pharmacology, Faculty of Dental Science, Kyushu University, Fukuoka 812-8582, Japan

[b]Section of Orthodontics and Dentofacial Orthopedics, Division of Oral Health, Growth and Development, Faculty of Dental Science, Kyushu University, Fukuoka, Japan

[c]Center of Implant Dentistry, School of Stomatology, China Medical University, Shenyang 110002, China

[d]The VIP Department, School of Stomatology, China Medical University, Shenyang 110002, China

[e]Division of Frontier Life Science, Department of Medical and Dental Sciences, Graduate School of Biomedical Sciences, Nagasaki University, Nagasaki, 852-8588, Japan.

[f]Section of Geriatric Dentistry and Perioperative Medicine in Dentistry, Division of Maxillofacial Diagnostic and Surgical Sciences, Faculty of Dental Science, Kyushu University, Fukuoka 812-8582, Japan

[g]OBT Research Center, Faculty of Dental Sciences, Kyushu University, Fukuoka 812-

8582, Japan

[h]Key Laboratory of Molecular Medicine and Biotherapy, Department of Biology, School of Life Science, Beijing Institute of Technology, Haidian District, Beijing 100081, China.

Running Title: Linking Periodontitis and Alzheimer's disease

*Correspondence

Zhou Wu, PhD. Department of Aging Science and Pharmacology, OBT Research Center, Faculty of Dental Science, Kyushu University, Fukuoka 812-8582, Japan. TEL/FAX: +81 92 642 6414; Email: zhouw@dent.kyushu-u.ac.jp

Junjun Ni, Ph.D. Key Laboratory of Molecular Medicine and Biotherapy, Department of Biology, School of Life Science, Beijing Institute of Technology, Haidian District, Beijing 100081, China. TEL: +86 17600397519; Email: nijunjun@bit.edu.cn

ABSTRACT

Background: Studies have reported that synaptic failure occurs before the Alzheimer's disease (AD) onset. The systemic *Porphyromonas gingivalis* (*P. gingivalis*) infection is involved in memory decline. We previously showed that leptomeningeal cells, covering the brain, activate glial cells by releasing IL-1β in response to systemic inflammation. **Objective:** In the present study, we focused on the impact of leptomeningeal cells on neurons during systemic *P. gingivalis* infection. **Methods:** The responses of leptomeningeal cells and cortical neurons to systemic *P. gingivalis* infection were examined in 15-month-old mice. The mechanism of IL-1β production by *P. gingivalis* infected leptomeningeal cells was examined, and primary cortical neurons were treated with *P. gingivalis* infected leptomeningeal cells condition medium (*Pg* LCM). **Results:** Systemic *P. gingivalis* infection increased the expression of IL-1β in leptomeninges and reduced the synaptophysin (SYP) expression in leptomeninges proximity cortex in mice. Leptomeningeal cells phagocytosed *P. gingivalis* resulting in lysosomal rupture and cathepsin B (CatB) leakage. Leaked CatB mediated NLRP3 inflammasome activation inducing IL-1β secretion in leptomeningeal cells. *Pg* LCM decreased the expression of synaptic molecules, including SYP, which was inhibited by an IL-1 receptor antagonist pre-treatment. **Conclusion:** These observations demonstrate that *P. gingivalis* infection is involved in synaptic failure by inducing CatB/NLRP3 inflammasome-mediated IL-1β production in leptomeningeal cells. The periodontal bacteria-induced synaptic damage may accelerate the onset and cognitive decline of AD.

Keywords: *Porphyromonas gingivalis*, Leptomeningeal cells, Alzheimer's disease, Inflammasome, Cathepsin B, Interleukin-1 beta, Synapses

ABBREVIATIONS:

AD, Alzheimer's disease; BCSFB, blood-cerebrospinal fluid barrier; BDNF, brain-derived neurotrophic factor; CatB, cathepsin B; CREB, cAMP response element-binding protein; CSF, cerebrospinal fluid; Cyto D, cytochalasin D; IκBα, inhibitor of nuclear factor kappa B; LAMP2, lysosome-associated membrane protein 2; *Pg*LPS, lipopolysaccharide from *Porphyromonas gingivalis*; MCI, mild cognitive impairment; MOI, multiplicity of infection; NF-κB, nuclear factor kappa B; NLRP3, NOD-, LRR- and pyrin domain-containing protein 3; p-CREB, phosphorylated cAMP response element-binding protein; *P. gingivalis*, *Porphyromonas gingivalis*; *Pg* LCM, *Porphyromonas gingivalis* infected leptomeningeal cells condition medium; SYN1, synapsin1; SYP, synaptophysin; VGLUT1, vesicular glutamate transporter1

INTRODUCTION

The rate of Alzheimer's disease (AD), the most prevalent type of dementia, is increasing with the global elderly population growing. Since no effective treatment of AD has been established yet, it is extremely important to identify early risk factors for delaying the onset and pathological progression of AD [1].

Synaptic failure occurs before the onset of AD and is closely associated with the observation of a cognitive decline in AD patients [2,3]. It was reported that the expression of synaptic molecules, such as synaptophysin (SYP), vesicular glutamate transporter1(VGLUT1), and synapsin1 (SYN1) reduced in the brain of patients with mild cognitive impairment (MCI) and AD [4,5]. In addition, growing evidence suggests deficits in brain-derived neurotrophic factor (BDNF) signaling, a major regulatory pathway for synaptic generation and plasticity [6,7], contribute to the pathogenesis of neurodegenerative disorders, including AD [8].

Periodontitis, the most common oral dysbiosis-induced inflammatory gum disease in adults, has drawn attention as a risk factor for AD [9]. The morbidity of periodontitis is positively correlated with the onset and pathological progression of AD [9,10]. *Porphyromonas gingivalis (P. gingivalis)*, a keystone pathogen of periodontitis, is recognized as the major linking factor between periodontitis and AD[11]. In addition, *P. gingivalis* DNA and its virulence factors, including lipopolysaccharide (LPS) and gingipain, have been detected in the cortex and cerebrospinal fluid (CSF) of AD patients [12,13].

Recently, preclinical studies have suggested that periodontitis may contribute to

AD onset, since exposure to *P. gingivalis*, *P. gingivalis* LPS as well as gingipain induced the hallmarks of AD-like pathologies, including amyloid β (Aβ) accumulation, neuroinflammation and memory decline in mice [14–16]. Furthermore, we recently found that the memory decline induced by *P. gingivalis* occurred earlier than *P. gingivalis* LPS in middle-aged mice [14,15]. However, the involvement of *P. gingivalis* in the synaptic changes remains unclear.

The leptomeninges, the innermost layer of the meninges, anatomically envelop the brain and spinal cord [17,18]. As the interfaces between systemic circulation and the brain, leptomeningeal cells respond to systemic inflammatory pathogens to produce pro-inflammatory mediators and induce neuroinflammation [17–20]. In addition to forming a physical barrier (the blood-cerebrospinal fluid barrier [BCSFB]), leptomeningeal cells are known to constantly produce and secrete soluble factors that directly affect neurons [21–23]. Bacteraemia may induce meningitis which can lead to neuronal injury [24]. Although almost all pathogenic bacteria have the potential to induce meningitis [24], different bacteria induce distinct inflammatory responses [25]. In addition, we previously showed that *P. gingivalis* LPS induces TNF-α production by leptomeningeal cells [20]. This observation prompted us to explore the response of leptomeningeal cells after *P. gingivalis* infection.

As a master pro-inflammatory cytokines for inducing the pathogenesis of AD, IL-1β has been accepted to induce synapse failure [26,27]. It is well known that NOD-, LRR- and pyrin domain-containing protein 3 (NLRP3) inflammasome activation mediates the IL-1β production in response to infectious microbes, including *P.*

gingivalis [28,29]. In addition, cathepsin B (CatB), a cysteine lysosomal protease, has been shown to perform a mediating role in IL-1β production in response to different stimulations [30,31].

We hypothesized that leptomeningeal cells are involved in synaptic failure by releasing soluble factors during *P. gingivalis* infection. In the present study, we tested our hypothesis by identifying that leptomeningeal cell-produced IL-1β induced synaptic failure during *P. gingivalis* infection.

MATERIALS AND METHODS

Animals

Fifteen-month-old female mice on a C57/BL6J background (Japan SLC, Incorporation, Japan) maintained in a specific-pathogen-free condition were used. All animal treatments were under the protocols approved by the Institutional Animal Care and Use Committee of Kyushu University. The sample size determination was based on the behavior test data of our previous publication [15]. The mice (n = 6 each group) were intraperitoneally injected with *P. gingivalis* (1×10^8 CFU/mouse) in 100 μl phosphate-buffered saline (PBS) every 3 days for three consecutive weeks as the *P. gingivalis*-infected mice. The age-matched mice (n = 6) were intraperitoneally injected with 100 μl PBS in the same time course as the controls.

Bacteria culture

Porphyromonas gingivalis ATCC 33277, a typical avirulent stain, is widely used to set

up *P. gingivalis* infection models [32–34]. *P. gingivalis* ATCC 33277 was cultured on a blood BHI (brain heart infusion) agar plate containing 40 mg/ml trypot-soya agar (Nissui Pharmaceutical co., Ltd. Tokyo, Japan), 5 mg/ml BHI (Becton, Dickinson and Company, Franklin Lakes, NJ, USA), 1 g/ml cysteine (Wako Pure Chemical Industries, Osaka, Japan), 5 μg/ml hemin (Sigma-Aldrich, St. Louis, MO, USA), 1 μg/ml menadione (Sigma-Aldrich), 5% defibrinated sheep blood (Nippon Bio-test laboratories, Tokyo, Japan) in bactron anaerobic chamber (Shel Lab, Cornelius, OR, USA) with mix gas of 10% CO_2, 10% H_2, 80% N_2. *P. gingivalis* was grown in BHI medium containing 37 mg/ml BHI, 2.5 mg/ml yeast extract (Becton, Dickinson and Company), 1 g/ml cysteine, 5 μg/ml hemin, and 1 μg/ml menadione. *P. gingivalis* was pelleted by centrifuge at 6000×*g* and suspended by neurobasal maintenance medium (Thermo Fisher Scientific, Tokyo, Japan) or Dulbecco's Modified Eagle Medium (DMEM, Nissui Pharmaceutical co., Ltd.) containing 10% fetal bovine serum (Invitrogen, San Diego, CA, USA) and 1% penicillin-streptomycin (Invitrogen) before treatment in cell culture. *P. gingivalis* was suspended by 100 μl PBS for in *vivo* experiments. To trace the *P. gingivalis* in phagocytosis, *P. gingivalis* was fluorescence-labeled by 10 μM CFDA SE (Vybrant CFDA SE Cell Tracer Kit, Invitrogen), a cell tracer kit. According to the manufacturer protocol, *P. gingivalis* in BHI medium was pelleted by centrifuge and the supernatant was aspirated. Then, the pelleted *P. gingivalis* was resuspended in PBS containing the probe and incubated for 15 min. at 37°C. The probe incubated *P. gingivalis* was re-pellet by centrifugation and resuspend in a fresh BHI medium. Incubated the *P. gingivalis* for another 30 min., which could ensure

complete modification of the probe, according to the manufacturer protocol. Finally, the incubated *P. gingivalis* was washed 3 times by PBS and used to infect the leptomeningeal cells.

Cell culture

Leptomeningeal cells were prepared from the postnatal day one (P1) mice brain on the background of C57black/6N mouse. Leptomeningeal tissues were cut into small pieces and plated on poly-D-lysine (Thermo Fisher Scientific) coated culture dishes, incubated in Minimum Essential Medium Eagle (MEM, Nissui Pharmaceutical co., Ltd.) containing 10% fetal bovine serum (Invitrogen), 10 μg/ml insulin, 1% penicillin-streptomycin (Invitrogen) and 2 mg/ml glucose (Invitrogen) under 37 °C and 5% CO_2 in a humid atmosphere. For conditional medium collection, MEM was replaced by neurobasal maintenance medium (Thermo Fisher Scientific) or Dulbecco's Modified Eagle Medium (DMEM, Nissui Pharmaceutical co., Ltd.) before infection with *P. gingivalis*.

Primary cortex neurons were prepared from the postnatal day one (P1) mice brain on the background of C57black/6N mouse. Dissected brain tissues were enzymatic digestion with a Neural Tissue Dissociation kit (Miltenyi Biotec). The separated neurons were kept in an attachment medium for 24 h and then replaced with a neurobasal maintenance medium (Thermo Fisher Scientific) containing 10% fetal bovine serum (Invitrogen) and 1% penicillin-streptomycin (Invitrogen). The cells were seeded at a density of 1.25×10^6 cells/ml for biochemical assay, 2×10^5 cells/ml for

immunohistochemistry. Arabinosylcytosine (Ara-C, Sigma-Aldrich) was added under 5 μM on 3rd day out of *in vitro*. In the conditional medium incubation experiments, the leptomeningeal cell medium was replaced by neurobasal maintenance medium (Thermo Fisher Scientific) before infection with *P. gingivalis*.

Mouse neuroblastoma N2a cells purchased from American Type Culture Collection (Manassas, VA, USA) were cultured in Dulbecco's Modified Eagle Medium (DMEM, Nissui Pharmaceutical co., Ltd.) containing 10% fetal bovine serum (Invitrogen), 10 μg/ml insulin, 1% penicillin-streptomycin (Invitrogen) and 2 mg/ml glucose (Invitrogen) under 37 °C and 5% CO_2 in a humid atmosphere. The cells were seeded at a density of 2×10^5 cells/ml for western blotting or immunohistochemistry.

Reagents

Cathepsin B inhibitor CA-074Me was purchased from Peptide institute, INC. (Osaka, Japan). NLRP3 siRNA was purchased from Thermo Fisher Scientific. Cytochalasin D (Cyto D) was purchased from Sigma-Aldrich. IL-1β receptor antagonist IL-1Ra was purchased from Cayman Chemical Company (Ann Arbor, MI, USA). Human BDNF was purchased from Sigma-Aldrich.

Cell viability assay

Leptomeningeal cells were seeded in 96-well plates for 24 h (5000 cells/well) and were infected with 1, 5, and 10 multiplicity of infection (MOIs) of *P. gingivalis*. Primary neurons were seed in 96-well plates for 2 weeks (5000 cells/well) and were incubated

with LCM for 24 h. Cell viability was measured by Cell-Counting Kit-8 (CCK-8, Dojindo, Kumamoto, Japan) according to the manufacturer's protocol. At different time points, 10 μl CCK-8 solution was added to each well and incubated for 1 h. The absorbance at 450 nm was measured by a microplate reader.

NLRP3 knockdown with small interfering RNAs

Leptomeningeal cells were seeded in 6-well plates in MEM one day before and were transiently transfected with NLRP3 siRNA (169997, Thermo Fisher Scientific) according to the manufacturer protocol. First, 30 pmol siRNA with 250 μl Opti-MEM was mixed. Second, 5 μl RNA iMAX was added to 250 μl Opti-MEM. Then, these two mixtures were combined and incubated for 10 min. Finally, the solution was added to each well and mix well. *P. gingivalis* was applied to the leptomeningeal cells after treatment with NLRP3 siRNA for 36 h. The cells and condition medium were collected at 3 h for western blot and neuron treatment. The efficiency of transfection was examined by real-time quantitative polymerase chain reaction.

Immunofluorescent imaging

Mice were anesthetized and sacrificed by intracardiac perfusion with PBS. The brain was extracted following immersed in 4% PFA at 4℃ overnight and cryoprotected in 30% sucrose in PBS for 2 days then embedded in the optimal cutting temperature (OCT) compound (Sakura Finetek Japan Co., Ltd. Tokyo, Japan). The serial coronal frozen sections (14 μm thick) were prepared for immunofluorescent staining as reported

previously [14]. The sections were washed with PBS for 10 min at room temperature and incubated with antibody dilution buffer (1% BSA and 0.4% TritonX-100 in PBS) at 4℃ overnight and then with the primary antibodies in antibody dilution buffer at 4℃ for 2 days as follows: mouse anti-fibronectin (1:1000; novusbio, Japan), goat anti-IL-1β (1:1000; R&D), rabbit anti-synaptophysin (SYP, 1:1000; Abcam). After washing with PBS, the sections were incubated with secondary antibodies in antibody dilution buffer at room temperature for 2 h as follows: donkey anti-mouse Cy3 (1:1000; Jackson ImmunoResearch), donkey anti-goat Alexa 488 (1:1000; Jackson ImmunoResearch), donkey anti-rabbit Alexa 488 (1:1000; Jackson ImmunoResearch). The sections were then incubated with Hoechst in antibody dilution buffer (1:200; Sigma-Aldrich) and mounted in Vectashield anti-fading medium (Vector Laboratories, CA, USA). Fluorescence images were taken using a CLSM (C2si, Nikon, Japan). For the relative immunoreactivity calculation, the space within 50 μm of fibronectin-positive leptomeningeal cells was defined as the leptomeninges proximity cortex. The fluorescent intensity of SYP was measured in these sections and the fluorescent intensity of IL-1β was measured in the fibronectin-positive leptomeningeal cells sections. The fluorescent intensity was determined relative to the selected area size.

The leptomeningeal cells and neurons were seeded on PEI-coated glasses in 24-well plates. For primary neuron staining, 30% cell medium was replaced by leptomeningeal cells medium with or without *P. gingivalis* treatment. For N2a cells CREB activity, BDNF was administrated 2 h and IL-1Ra was administrated 1 h following the LCM treatment. The cells were fixed with 4% paraformaldehyde. After

washing the cells with PBS twice, they were incubated with rabbit anti-LAMP1 (1:1000; Abcam), MAP2 (1:1000; Millipore), Phospho-CREB (1:1000, Cell Signal) overnight at 4°C and incubated with anti-rabbit Alexa Cy3 (1:2000; Jackson ImmunoResearch) at room temperature for 2 h then incubated with Hoechst (1:200; Sigma-Aldrich). For AO staining, leptomeningeal cells were infected with *P. gingivalis* for 2 h and CV-Cathepsin B Detection Kit (Enzo, Switzerland) was used following the manufacturer protocol. Images were collected by a fluorescence microscope (C2si; Nikon). Image J software (64-bit Java 1.8.0 112, NIH) was used to calculate the neurite length and fluorescent density. For the p-CREB relative immunoreactivity calculation, the total immunofluorescence was measured in each microscopic field of view, and the number of cell nuclei was also counted. The relative immunoreactivity is the total immunofluorescence relative to the number of cell nuclei and the control relative immunofluorescence was set up at one.

Real-time quantitative polymerase chain reaction (qRT-PCR)

The mRNA was isolated from the leptomeningeal cells and neurons at various time points. The total RNA was extracted using the RNAiso Plus (Takara) according to the manufacturer's instructions. A total of 2 μg extracted RNA was reverse transcribed to cDNA using the ReverTra Ace qPCR RT Master Mix (TOYOBO). After an initial denaturation step at 95°C for 1 min, temperature cycling was initiated. Each cycle consisted of denaturation at 95°C for 10 s, annealing at 60°C for the 30 s, and elongation for 30 s. In total, 40 cycles were performed. The cDNA was amplified in duplicate using

a THUNDERBIRD SYBR qPCR Mix (TOYOBO) with a Corbett Rotor-Gene RG-3000A Real-Time PCR System (Sydney, Australia). The data were evaluated using the RG-3000A software program (version Rotor-Gene 6.1.93, Corbett). The sequences of primer pairs were as follows: NLRP3, 5'-ACAAGCCTTTGCTCCAGACCCTAT-3' and 5'-TGCTCTTCACTGCTATCAAGCCCT-3'; Caspase-1, 5'-CTTGTTTCTCTCCACGGCA-3' and 5'-TCCAGGAGGGAATATGTGG-3'; CatB, 5'-GCAGCCAACTCTTGGAACCTT-3' and 5'-GGATTCCAGCCACAATTTCTG-3'; IL-1β, 5'-CAACCAACAAGTGATATTCTCCATG-3' and 5'-GATCCACACTCTCCAGCTGCA-3'; Synapsin I, 5'-GGTCTTCCAGTTACCCGACA-3' and 5'-CAGCACAACATACCCTGTGG-3'; synaptophysin: 5'-AGGTGCTGCAGTGGGTCTTTGC-3' and 5'-CCCCTTTAACGCAGGAGGGTGC-3'; VGLUT1, 5'-CCCCAAATCCTTGCACTTT-3' and 5'-AACAAATGGCCACTGAGAAACC-3'"; BDNF, 5'-AAAATGCTCACATCCA-3' and 5'-GAACAAATGCTGGTCTT-3'. For data normalization, an endogenous control (Actin) was assessed to control for the cDNA input, and the relative units were calculated by the comparative Ct method. The experiments were repeated three times, and the results are presented as the means of the ratios±standard error of the mean (SEM).

Immunoblotting analyses

The immunoblotting analyses were conducted as described previously [15]. The specimens were electrophoresed with 12% SDS-polyacrylamide gels and transferred to

nitrocellulose membranes by electrophoresis. Following the blocking, the membranes were incubated at 4°C overnight under gentle agitation with each primary antibody: goat anti- IL-1β (1:1000, R&D), mouse anti-caspase-1 (1:1000; AdipoGen), goat anti-CatB (1:1000; Santa Cruz Biotechnology), mouse anti-IκBα (1:1000; Cell Signaling), rabbit anti-Synaptophysin (1:20000; Abcam), rabbit anti-Phospho-CREB (1:1000, Cell Signal), rabbit anti-total CREB (1:1000, Cell Signal). After washing with PBS 3 times, the membranes were incubated with HRP-labeled anti-goat (1:2000; GE Healthcare), anti-mouse (1:2000; R&D Systems), anti-rabbit (1:2000; GE Healthcare), and mouse anti-actin (1:5,000, Abcam) for 2 h at room temperature. Following washing with PBS 3 times, the HRP-labeled protein bands were detected by an enhanced chemiluminescence detection system (ECL kit; GE Healthcare) with an image analyzer (LAS-1000; Fuji Photo Film).

ELISA

The *P. gingivalis* infected leptomeningeal cells medium was collected at indicated time points and used IL-1β enzyme-linked immunosorbent assay (R&D Systems) to measure the released IL-1β following the protocol provided by the manufacturer. The absorbency at 450 nm was measured using a microplate reader.

Statistical analyses.

The data are represented as the means ± SEM. The statistical analyses were performed by unpaired *t*-test, multiple *t*-test, and correlation using the GraphPad Prism software

package (GraphPad Software, California, USA). A value of $p < 0.05$ and a value of Q (desired FDR) < 5% was considered to indicate statistical significance.

RESULTS

The expression of IL-1β and SYP in middle-aged mice after systemic P. gingivalis infection

We first examined synaptic failure *in vivo* by staining synaptophysin (SYP), which is a major synaptic marker. The SYP immunoreactivity was significantly decreased in the cortex; this decrease was localized proximally to the leptomeninges in our mouse model (Fig. 1A, B, ***$p = 0.0003$ by unpaired *t*-test). The IL-1β immunoreactivity was also significantly increased in the fibronectin-positive leptomeningeal cells (Fig. 1C, D, ***$p < 0.0001$ by unpaired *t*-test). A correlation analysis indicated a negative correlation between IL-1β and SYP (Fig. 1E, r = -0.5424, $p = 0.0135$). These results indicate that leptomeningeal cell-produced IL-1β was associated with the decrease in SYP in middle-aged mice after *P. gingivalis* infection.

NLRP3 inflammasome activation in P. gingivalis-infected leptomeningeal cells

In an *in vitro* study, we first examined the cell viability of leptomeningeal cells infected by *P. gingivalis*. The cell viability of the leptomeningeal cells was not decreased up to 12 h at MOIs of 1, 5, or 10 (Fig. 2A). Therefore, an MOI of 10 was used in subsequent experiments. In comparison to the start culture time (0 h), the secretion of IL-1β was significantly increased from 1 h, peaked at 3 h, and was reduced at 6 and 12 h after *P.*

gingivalis infection (Fig. 2B, ***p* = 0.004268, *q* = 0.004310; ****p* < 0.000001, *q* < 0.000001 by multiple *t*-test). We next examined the involvement of NLRP3 inflammasome in IL-1β production after *P. gingivalis* infection. The mRNA expression of NLRP3 was significantly increased in the leptomeningeal cells from 1 h to 12 h after *P. gingivalis* infection (Fig. 2C, ****p* = 0.000002, *q* = 0.000002; ****p* = 0.000117, *q* = 0.000119; ****p* < 0.000001, *q* < 0.000001; ****p* = 0.000059, *q* = 0.000059 by multiple *t*-test). The knockdown of NLRP3 were conducted to further confirmed the involvement of NLRP3 inflammasome in the IL-1β production. The mRNA expression of NLRP3 was reduced in both *P. gingivalis* infected and uninfected cells (Fig. 2D, ****p* = 0.000173, *q* = 0.000174; ****p* = 0.000826, *q* = 0.000868; ***p* = 0.001123, *q* = 0.001134 by multiple *t*-test). The protein expression of mature caspase-1 was significantly increased at 3 h and decreased by NLRP3 siRNA (Fig. 2E, F, ****p* = 0.000018, *q* = 0.000018; ††*p* = 0.005887, *q* = 0.005946 by multiple *t*-test). The mature IL-1β was induced at 3 h and reversed by NLRP3 siRNA (Fig. 2G, H, ****p* = 0.000002, *q* = 0.000002; ††*p* = 0.001940, *q* = 0.001959 by multiple *t*-test). The *P. gingivalis* infection-induced IL-1β secretion was also reduced by NLRP3 siRNA (Fig. 2I, ****p* < 0.000001, *q* < 0.000001; ††*p* = 0.000080, *q* = 0.000080 by multiple *t*-test). These observations showed that NLRP3 inflammasome activation was involved in IL-1β secretion by leptomeningeal cells after *P. gingivalis* infection.

Involvement of CatB in NLRP3 inflammasome activation in P. gingivalis-infected leptomeningeal cells

We next examined the involvement of CatB in NLRP3 inflammasome activation in leptomeningeal cells after *P. gingivalis* infection, as CatB is required for NLRP3 inflammasome activation to product IL-1β [28,29]. Fluorescent-labeled *P. gingivalis* was detected in the lysosome-associated membrane protein 2 (LAMP2)-positive lysosomes, and the size of the lysosomes was enlarged in leptomeningeal cells at 1 h after *P. gingivalis* infection (Fig. 3A). The number of *P. gingivalis* in lysosomes was decreased by cytochalasin D (Cyto D), a specific phagocytosis inhibitor (Fig. 3A). The punctate acridine orange aggregates were decreased by 2 h after *P. gingivalis* infection (Fig. 3B). These results indicate that lysosomal damage was induced in leptomeningeal cells after *P. gingivalis* was phagocytized. Compared with the control cells, the protein expression of CatB in the cytosol was significantly increased at 2 h after *P. gingivalis* infection (Fig. 3C, D, $^{**}p = 0.009838$, $q = 0.009936$ by unpaired *t*-test). These findings suggest that *P. gingivalis* was phagocytized into lysosomes, which may interfere with the maintenance of lysosome integrity and result in CatB leakage into the cytosol.

The involvement of cytosol CatB in NLRP3 inflammasome activation was subsequently examined. The protein expression of mature-caspase-1 was significantly increased at 3 h after *P. gingivalis* infection. Pre-treatment with CA-074Me, the CatB specific inhibitor, significantly decreased the *P. gingivalis*-induced caspase-1 activation (Fig. 3E, F, $^{***}p = 0.000018$, $q = 0.000018$; $\dagger\dagger\dagger p = 0.000186$, $q = 0.000188$ by multiple *t*-test) and *P. gingivalis*-induced IL-1β secretion (Fig. 3G, $^{***}p < 0.000001$, $q < 0.000001$; $\dagger\dagger\dagger p = 0.000019$, $q = 0.000019$ by multiple *t*-test). The effect of *P. gingivalis* phagocytosis on IL-1β production was further examined. Pre-treatment with Cyto D

significantly inhibited the protein expression of mature IL-1β (Fig. 3H, I, ***p = 0.000632, q = 0.000639; ††p = 0.007640, q = 0.007716 by multiple t-test) as well as IL-1β secretion (Fig. 3J, ***p < 0.000001, q < 0.000001; †††p = 0.000002, q = 0.000002 by multiple t-test).

These observations showed that engulfment of *P. gingivalis* into lysosomes induced lysosome rupture and CatB leakage, which activated NLRP3 inflammasomes, resulting in secretion of IL-1β from leptomeningeal cells.

Involvement of CatB in the activation of NF-κB in P. gingivalis-infected leptomeningeal cells

CatB was reported to activate nuclear factor kappa B (NF-κB) through degradation of the inhibitor of NFκBα (IκBα) [14,15,31]. NF-κB activation is essential for upregulating the inflammasome components including NLRP3, caspase-1, and pro-IL-1β [36]. Therefore, we examined the involvement of CatB in NF-κB activation in leptomeningeal cells after *P. gingivalis* infection. Compared with the cells at 0 h, the CatB protein expression was significantly increased from 0.5 h to 3 h after *P. gingivalis* infection (Fig. 4A, B, ***p = 0.000378, q = 0.000382; *p = 0.018894, q = 0.019083; **p = 0.007366, q = 0.007440; ***p = 0.000333, q = 0.000336 by multiple t-test). Simultaneously, the expression of IκBα was significantly decreased at 1 h after *P. gingivalis* infection which was inhibited by CA-074Me (Fig. 4C, D, **p = 0.001098, q = 0.001109; †p = 0.030107, q = 0.030408 by multiple t-test).

We further observed that the *P. gingivalis* infection-induced increase in the

mRNA expression of NLRP3, Caspase-1, and IL-1β was significantly inhibited by pre-treatment with CA-074Me in leptomeningeal cells (Fig. 4E-G, ***p = 0.000851, q = 0.000860; †††p = 0.000070, q = 0.000070; ***p = 0.000653, q = 0.000660; †††p = 0.000443, q = 0.000448; ***p = 0.000078, q = 0.000079; †††p = 0.000716, q = 0.000723 by multiple t-test). Moreover, the *P. gingivalis*-induced increase in protein expression of both pro-IL-1β and mature IL-1β was also inhibited by CA-074Me (Fig. 4H-J, ***p = 0.000068, q = 0.000069; †p = 0.020663, q = 0.020870; ***p = 0.000653, q = 0.000660; †††p = 0.000443, q = 0.000448 by multiple t-test).

These observations showed that CatB promotes the activation of NF-κB to generate the molecules required for IL-1β production.

Involvement of P. gingivalis-infected leptomeningeal cells in synaptic molecules in neurons

As SYP was decreased in the cortex proximal to the leptomeningeal cells in *P. gingivalis*-infected mice, we developed a cellular model to investigate the influence of *P. gingivalis*-infected leptomeningeal cells on synaptic molecules in the cortical neurons. The conditioned medium of *P. gingivalis*-infected leptomeningeal cells (*Pg* LCM, 3 h after *P. gingivalis* infection) was applied to primary cultured cortical neurons. The cell viability of the primary cortical neurons was not reduced by applying 30% *Pg* LCM for 24 h (Fig. 5A). The mean neurite length was significantly reduced by the *Pg* LCM, showing that *Pg* LCM is involved in the morphological features of primary cortical neurons without inducing neuron death (Fig. 5B, C, **p = 0.002257 by

unpaired *t*-test). Therefore, 30% *Pg* LCM was used in the subsequent experiments.

Compared with the control neurons, the mRNA expression of synaptic markers, including SYP, VGLUT1 and SYN1, was significantly decreased by *Pg* LCM in primary cortical neurons (Fig. 5D, $^{**}p = 0.0011$; $^{**}p = 0.0088$; $^{***}p = 0.0005$ by unpaired *t*-test). The mRNA expression of SYP, VGLUT1 and SYN1 in *Pg* LCM-treated primary cortical neurons was significantly and negatively correlated with the concentration of IL-1β in *Pg* LCM (Fig. 5E, r = -0.8635, $p = 0.0267$; r = -0.8628, $p = 0.0270$; r = -0.9066, $p = 0.0127$). The protein expression of SYP was dramatically decreased by *Pg* LCM, which was significantly inhibited by pre-treatment with NLRP3 siRNA or CA-074 Me (Fig. 5F, G, $^{***}p = 0.000024$, $q = 0.000024$; $^{\dagger}p = 0.042422$, $q = 0.042846$; $^{\dagger\dagger\dagger}p = 0.000325$, $q = 0.000328$ by multiple *t*-test). The *Pg* LCM-induced reduction in the protein expression of SYP was dramatically inhibited by pre-treatment with IL-1 receptor antagonist (IL-1Ra) (Fig. 5H, I, $^{***}p = 0.000066$, $q = 0.000066$; $^{\dagger\dagger\dagger}p = 0.000010$, $q = 0.000011$ by multiple *t*-test).

These observations showed that secreted IL-1β from *P. gingivalis* infected leptomeningeal cells induced synaptic failure.

Involvement of P. gingivalis-infected leptomeningeal cells in BDNF/CREB signaling in neurons

To further explore the effect of IL-1β secreted by *P. gingivalis*-infected leptomeningeal cells on neurons, we focused on BDNF/CREB signaling, a major regulatory pathway for synaptic generation and plasticity in neurons [6,7]. The nuclear localization of

phosphorylated CREB (p-CREB) was first examined. The nuclear p-CREB was significantly increased at 4 h in BDNF pre-treated N2a cells; this was reduced by pre-treatment with *Pg* LCM (Fig. 6A, B, ***p = 0.000222, q = 0.000225; **p = 0.001939, q = 0.001958 by multiple t-test). IL-1Ra treatment reversed the *Pg* LCM-induced nuclear localization of p-CREB (Fig. 6A, B, *p = 0.046066, q = 0.046526 by multiple t-test). In addition, the *Pg* LCM-induced decrease in p-CREB was significantly reversed by pre-treatment with IL-1Ra (Fig. 6C, D, **p = 0.002569, q = 0.002595; **p = 0.005267, q = 0.005319; *p = 0.012384, q = 0.012508 by multiple t-test). Taken together, IL-1β from *P. gingivalis*-infected leptomeningeal cells suppress the BDNF/CREB signaling in neurons.

DISCUSSION

The major findings of the present study were that *P. gingivalis* infection activated CatB/NLRP3 inflammasome in leptomeningeal cells to induce the secretion of IL-1β, resulting in synaptic failure of cortical neurons (Summarized in Fig. 7). First, systemic *P. gingivalis* infection increased the expression of IL-1β in leptomeninges and reduced the SYP expression in leptomeninges proximity cortex in mice. Second, *P. gingivalis* infection activated NLRP3 inflammasome for IL-1β secretion by leptomeningeal cells. Third, CatB was involved in the activation of NF-κB, which is essential for pro-IL-1β production, as well as NLRP3 inflammasome. Fourth, secreted IL-1β from *P. gingivalis* infected leptomeningeal cells induced synaptic failure in cortical neurons. Taken together, this is the first study showing the involvement of leptomeningeal cells in

synaptic failure during *P. gingivalis* infection, thus providing a new mechanism underlying the involvement of periodontal bacterial infection in the initiation and pathological processes of AD.

Several strains of *P. gingivalis* have been identified, including ATCC33277 and W83. They are classified into virulent and avirulent strains [37]. ATCC33277 is a typical avirulent strain that is widely used to establish *P. gingivalis* infection models [38,39]. Other Gram-negative bacteria, like *E. coli*, and Gram-positive bacteria, like *S. pneumoniae*, are studied more widely in leptomeningeal cells, as these bacteria can induce severe and varied inflammatory responses resulting in meningitis onset and neuronal injury [24,25]. While we only studied ATCC33277 in our present study, we believe that other *P. gingivalis* strains may induce different responses, as different bacteria induce distinct inflammatory responses in leptomeningeal cells [25]. The primary ecological niche of *P. gingivalis* is the gingival sulcus and periodontal pocket [40], *P. gingivalis* has been considered to directly enter the bloodstream through ulcerated crevicular or pocket epithelium surrounding the teeth [41]. The bacteria in the CSF that induce an inflammatory response by leptomeningeal cells come from the circulatory system [24]. Therefore, intraperitoneal injection of *P. gingivalis* in mice was used in the present study to mimic *P. gingivalis* directly entering the bloodstream and systemic spread. Systemic *P. gingivalis* infection in AD pathology was also explored in our previous studies. It was found that *P. gingivalis* up-regulates the expression of RAGE, a key molecule involved in Aβ influx, in cerebral endothelial cells [15], and the peripheral pools of Aβ expand during chronic systemic *P. gingivalis* infection [42].

Another study using orally administered *P. gingivalis* showed neurodegeneration and the formation of extracellular Aβ42 in young adult WT mice [43]. Since they used a different manner of inducing *P. gingivalis* infection and mice of a different age, their findings could be explored further in a mouse or other models of Alzheimer's disease.

As structures covering the surface of the brain, leptomeningeal cells are recognized as an interface between the systemic circulation and the brain [17,22,23]. The significant increase of IL-1β in the fibronectin-positive leptomeningeal cells in the middle-aged mice after systemic *P. gingivalis* infection (Fig.1C, D), suggesting that leptomeningeal cells are the important source of IL-1β for inducing neuroinflammation during systemic *P. gingivalis* infection. The secretion of IL-1β by primary leptomeningeal cells was detected as soon as 1 h and peaked at 3 h (Fig.2B), indicating leptomeningeal cells are sensitively responsive to *P. gingivalis* infection, similar with other bacteria [25]. The IL-1β secretion was mediated by NLRP3 inflammasome activation, as NLRP3 siRNA reduced the NLRP3 mRNA expression resulted in a significant reduction in the mature caspase-1 and IL-1β protein levels, as well as the secretion of IL-1β (Fig. 2). These observations in our cellular model were consistent with other cells' responses to *P. gingivalis* [28,29].

CatB, a cysteine lysosomal protease, is known to be involved in NLRP3 inflammasome activation [30]. In the present study, Cyto D, phagocytosis inhibitor, inhibited the *P. gingivalis*-induced upregulation of IL-1β secretion, thus indicating that the phagocytosis of *P. gingivalis* is required for production of IL-1β. This is consistent with the effects of phagocytosis on IL-1β production [30,31]. *P. gingivalis* was observed

in the lysosome and lysosomal damage resulted in CatB leakage into the cytosol. CA-074Me, the CatB specific inhibitor, significantly inhibited the upregulation of the mature caspase-1 protein expression, as well as IL-1β secretion by *P. gingivalis* infected leptomeningeal cells (Fig.3), demonstrating that CatB is involved in the IL-1β secretion by activating caspase-1 during *P. gingivalis* infection. The inhibitory rate of IL-1β secretion by CA-074Me was more than that by Cyto D, suggesting additional effects of CatB on IL-1β secretion by *P. gingivalis*-infected leptomeningeal cells.

CatB is known to be involved in the NF-κB activation [15,31,35]. In the present study, the *P. gingivalis*-induced decrease in IκBα was significantly reversed by CA-074Me, indicating that CatB promotes activation of NF-κB by degrading IκBα in *P. gingivalis*-infected leptomeningeal cells. The effects of CatB on degrading IκBα for NF-κB activation were supported by the findings of previous reports in other brain cells [15,35]. The CatB-NF-κB positive feedback loop may further accelerate NF-κB activation in leptomeningeal cells during *P. gingivalis* infection, as the CatB promoter contains NF-κB binding sites [44]. The promoters of NLRP3 and IL-1β have NF-κB binding sites [45,46], and NF-κB activation is sufficient to induce pro-caspase-1 [47]. The significant inhibition of CA-074Me occurs with the expression of NLRP3, caspase-1, and IL-1β suggesting that CatB-involved NF-κB activation contributes to the production of IL-1β by *P. gingivalis*- infected leptomeningeal cells.

Thus, CatB is involved in IL-1β secretion in two ways, one is promoting NF-κB signaling to product NLRP3, pro-caspase-1, and pro-IL-1β; the other is activating NLRP3 inflammasome to process pro-IL-1β to mature IL-1β in *P. gingivalis*-infected

leptomeningeal cells.

As the decrease in SYP accompanied the production of IL-1β in our mouse model of systemic *P. gingivalis* infection (Fig.1) and IL-1β has been accepted to induce synaptic failure, we focused on synaptic molecules in neurons as an outcome of *P. gingivalis*-induced IL-1β in our cellular models. The major synaptic proteins, including SYP, SYN1, and VGLUT1 were used to evaluate synaptic generation. A reduction in SYP is considered to reflect a reduction in the distribution of synapses in the brain [48], VGLUT1 is known to determine the amount of glutamatergic transmission [49], and a reduction in SYN1 induces the early disruption of synaptic generation [50]. In the present study, the mRNA expression of SYP, SYN1, as well as VGLUT1 in the primary cortical neurons, was reduced by *Pg* LCM treatment without inducing neuron death (Fig. 5). In addition, the expression of the synaptic molecules in primary cortical neurons showed a strong negative correlation with the concentration of IL-1β in *Pg* LCM, and the *Pg* LCM-induced SYP reduction in the protein level was prevented by IL-1Ra (Fig.5). These results strongly suggest that IL-1β is the major soluble factor in *Pg* LCM that induces synaptic failure. These results are consistent with other studies showing the involvement of IL-1β in downregulating synaptic molecules [51].

BDNF signaling is a major regulator of synaptic generation and plasticity [6,7]. In the present study, the BDNF-induced activation of CREB signaling was depressed by *Pg* LCM and the depression was reversed by pretreatment with IL-Ra, suggesting that *P. gingivalis*-infected leptomeningeal cells depressed the BDNF-induced activation of CREB signaling through the secretion of IL-1β. The *Pg* LCM IL-1β-induced

reduction in CREB signaling activation may also contribute to its downregulating effects on synaptic proteins, as the activation of CREB signaling is involved in the regulation of SYP and SYN1 [51].

In conclusion, we showed that the secretion of IL-1β was induced in *P. gingivalis*-infected leptomeningeal cells by CatB activating NLRP3 inflammasomes and NF-κB. The secreted IL-1β induced synaptic failure and blocked BDNF/CREB signaling in neurons.

These findings highlight a new mechanism underlying the involvement of periodontitis in AD initiation and suggest that CatB may be an early intervention therapeutic target for delaying the onset of AD during *P. gingivalis* infection.

ACKNOWLEDGMENTS

This work was supported by funding from Grants-in-Aid for Scientific Research, Japan (16K11478 to Z.W), the research grant for the OBT research center from Kyushu University (to Z.W), and Beijing Institute of Technology Research Fund Program for Young Scholars to J.N (2020CX04166).

Authors' contribution

W.H. conducted most of the experiments, analyzed the data and wrote the manuscript. F.Z., Y.G and M.J. analyzed the data. X.Z and X.Y. provided valuable advices. T.K. provided unpublished reagents/analytic tools. S.M. and H.K. provided valuable advices. J.N. designed the study and wrote the manuscript. Z.W. designed and supervised the experiments and wrote the manuscript. All authors read and approved the final

manuscript.

DISCLOSURE STATEMENT

The authors declare no conflicts of interest in association with the present study.

REFERENCES

[1] Cummings J, Lee G, Ritter A, Zhong K (2018) Alzheimer's disease drug development pipeline: 2018. *Alzheimer's Dement Transl Res Clin Interv* **4**, 195–214.

[2] Kordower JH, Chu Y, Stebbins GT, Dekosky ST, Cochran EJ, Bennett D, Mufson EJ (2001) Loss and atrophy of layer II entorhinal cortex neurons in elderly people with mild cognitive impairment. *Ann Neurol* **49**, 202–213.

[3] Selkoe DJ (2002) Alzheimer's disease is a synaptic failure. *Science* **298**, 789–791.

[4] Counts SE, Alldred MJ, Che S, Ginsberg SD, Mufson EJ (2014) Synaptic gene dysregulation within hippocampal CA1 pyramidal neurons in mild cognitive impairment. *Neuropharmacology* **79**, 172–179.

[5] Du X, Li J, Li M, Yang X, Qi Z, Xu B, Liu W, Xu Z, Deng Y (2020) Research progress on the role of type i vesicular glutamate transporter (VGLUT1) in nervous system diseases. *Cell Biosci* **10**, 1–10.

[6] Bramham CR, Messaoudi E (2005) BDNF function in adult synaptic plasticity: The synaptic consolidation hypothesis. *Prog Neurobiol* **76**, 99–125.

[7] Fritsch B, Reis J, Martinowich K, Schambra HM, Ji Y, Cohen LG, Lu B (2010) Direct current stimulation promotes BDNF-dependent synaptic plasticity: Potential implications for motor learning. *Neuron* **66**, 198–204.

[8] Bomba M, Granzotto A, Castelli V, Onofrj M, Lattanzio R, Cimini A, Sensi SL (2019) Exenatide Reverts the High-Fat-Diet-Induced Impairment of BDNF Signaling and Inflammatory Response in an Animal Model of Alzheimer's Disease. *J Alzheimer's Dis* **70**, 793–810.

[9] Kamer AR, Dasanayake AP, Craig RG, Glodzik-Sobanska L, Bry M, De Leon MJ (2008) Alzheimer's disease and peripheral infections: The possible contribution from periodontal infections, model and hypothesis. *J Alzheimer's Dis* **13**, 437–449.

[10] Ide M, Harris M, Stevens A, Sussams R, Hopkins V, Culliford D, Fuller J, Ibbett P, Raybould R, Thomas R, Puenter U, Teeling J, Perry VH, Holmes C (2016) Periodontitis and Cognitive Decline in Alzheimer's Disease. *PLoS One* **11**, e0151081.

[11] Hajishengallis G, Lamont RJ (2012) Beyond the red complex and into more complexity: The polymicrobial synergy and dysbiosis (PSD) model of periodontal disease etiology. *Mol Oral Microbiol* **27**, 409–419.

[12] Poole S, Singhrao SK, Kesavalu L, Curtis MA, Crean SJ (2013) Determining the presence of periodontopathic virulence factors in short-term postmortem Alzheimer's disease brain tissue. *J Alzheimer's Dis* **36**, 665–677.

[13] Dominy SS, Lynch C, Ermini F, Benedyk M, Marczyk A, Konradi A, Nguyen M,

Haditsch U, Raha D, Griffin C, Holsinger LJ, Arastu-Kapur S, Kaba S, Lee A, Ryder MI, Potempa B, Mydel P, Hellvard A, Adamowicz K, Hasturk H, Walker GD, Reynolds EC, Faull RLM, Curtis MA, Dragunow M, Potempa J (2019) *Porphyromonas gingivalis* in Alzheimer's disease brains: Evidence for disease causation and treatment with small-molecule inhibitors. Sci Adv **5**.

[14] Wu Z, Ni J, Liu Y, Teeling JL, Takayama F, Collcutt A, Ibbett P, Nakanishi H (2017) Cathepsin B plays a critical role in inducing Alzheimer's disease-like phenotypes following chronic systemic exposure to lipopolysaccharide from *Porphyromonas gingivalis* in mice. *Brain Behav Immun* **65**, 350–361.

[15] Zeng F, Liu Y, Huang W, Qing H, Kadowaki T, Kashiwazaki H, Ni J, Wu Z (2020) Receptor for advanced glycation end products up-regulation in cerebral endothelial cells mediates cerebrovascular-related amyloid β accumulation after *Porphyromonas gingivalis* infection. *J Neurochem jnc*.15096.

[16] Gu Y, Wu Z, Zeng F, Jiang M, Teeling JL, Ni J, Takahashi I (2020) Systemic Exposure to Lipopolysaccharide from *Porphyromonas gingivalis* Induces Bone Loss-Correlated Alzheimer's Disease-Like Pathologies in Middle-Aged Mice. *J Alzheimer's Dis* 1–14.

[17] Wu Z, Zhang J, Nakanishi H (2005) Leptomeningeal cells activate microglia and astrocytes to induce IL-10 production by releasing pro-inflammatory cytokines during systemic inflammation. *J Neuroimmunol* **167**, 90–98.

[18] Wu Z, Tokuda Y, Zhang XW, Nakanishi H (2008) Age-dependent responses of glial cells and leptomeninges during systemic inflammation. *Neurobiol Dis* **32**,

543–551.

[19] Vernet-der Garabedian B, Lemaigre-Dubreuil Y, Mariani J (2000) Central origin of IL-1β produced during peripheral inflammation: Role of meninges. *Mol Brain Res* 75, 259–263.

[20] Liu Y, Wu Z, Zhang X, Ni J, Yu W, Zhou Y, Nakanishi H (2013) Leptomeningeal cells transduce peripheral macrophages inflammatory signal to microglia in reponse to *Porphyromonas gingivalis* LPS. *Mediators Inflamm* 2013.

[21] Kipnis J (2016) Multifaceted interactions between adaptive immunity and the central nervous system. *Science* **353**, 766–771.

[22] Rua R, McGavern DB (2018) Advances in Meningeal Immunity. *Trends Mol Med* **24**, 542–559.

[23] King VR, Hewazy D, Alovskaya A, Phillips JB, Brown RA, Priestley J V. (2010) The neuroprotective effects of fibronectin mats and fibronectin peptides following spinal cord injury in the rat. *Neuroscience* **168**, 523–530.

[24] Kim KS (2003) Pathogenesis of bacterial meningitis: From bacteraemia to neuronal injury. *Nat Rev Neurosci* **4**, 376–385.

[25] Fowler MI, Weller RO, Heckels JE, Christodoulides M (2004) Different meningitis-causing bacteria induce distinct inflammatory responses on interaction with cells of the human meninges. *Cell Microbiol* **6**, 555–567.

[26] Mishra A, Kim HJ, Shin AH, Thayer SA (2012) Synapse loss induced by interleukin-1β requires pre-and post-synaptic mechanisms. *J Neuroimmune Pharmacol* **7**, 571–578.

[27] Voet S, Srinivasan S, Lamkanfi M, Loo G (2019) Inflammasomes in neuroinflammatory and neurodegenerative diseases. *EMBO Mol Med* **11**.

[28] Park E, Na HS, Song YR, Shin SY, Kim YM, Chung J (2014) Activation of NLRP3 and AIM2 inflammasomes by *Porphyromonas gingivalis* infection. *Infect Immun* **82**, 112–123.

[29] Okano T, Ashida H, Suzuki S, Shoji M, Nakayama K, Suzuki T (2018) *Porphyromonas gingivalis* triggers NLRP3-mediated inflammasome activation in macrophages in a bacterial gingipains-independent manner. *Eur J Immunol* **48**, 1965–1974.

[30] Halle A, Hornung V, Petzold GC, Stewart CR, Monks BG, Reinheckel T, Fitzgerald KA, Latz E, Moore KJ, Golenbock DT (2008) The NALP3 inflammasome is involved in the innate immune response to amyloid-β. *Nature Immun* **9**, 857-865

[31] Wu Z, Sun L, Hashioka S, Yu S, Schwab C, Okada R, Hayashi Y, McGeer PL, Nakanishi H (2013) Differential pathways for interleukin-1β production activated by chromogranin A and amyloid β in microglia. *Neurobiol Aging* **34**, 2715–2725.

[32] Ishida N, Ishihara Y, Ishida K, Tada H, Funaki-Kato Y, Hagiwara M, Ferdous T, Abdullah M, Mitani A, Michikawa M, Matsushita K (2017) Periodontitis induced by bacterial infection exacerbates features of Alzheimer's disease in transgenic mice. *Aging Mech Dis* **3**, 15.

[33] Sato K, Takahashi N, Kato T, Matsuda Y, Yokoji M, Yamada M, Nakajima T,

Kondo N, Endo N, Yamamoto R, Noiri Y, Ohno H, Yamazaki K (2017) Aggravation of collagen-induced arthritis by orally administered *Porphyromonas gingivalis* through modulation of the gut microbiota and gut immune system. *Sci Rep* **7**, 1–13.

[34] Haditsch U, Roth T, Rodriguez L, Hancock S, Cecere T, Nguyen M, Arastu-Kapur S, Broce S, Raha D, Lynch CC, Holsinger LJ, Dominy SS, Ermini F (2020) Alzheimer's Disease-Like Neurodegeneration in *Porphyromonas gingivalis* Infected Neurons with Persistent Expression of Active Gingipains. *J Alzheimer's Dis* **75**, 1301–1317.

[35] Ni J, Wu Z, Peterts C, Yamamoto K, Qing H, Nakanishi H (2015) The critical role of proteolytic relay through cathepsins B and E in the phenotypic change of microglia/macrophage. *J Neurosci* **35**, 12488–12501.

[36] Swanson K V., Deng M, Ting JPY (2019) The NLRP3 inflammasome: molecular activation and regulation to therapeutics. *Nat Rev Immunol* **19**, 477–489.

[37] Igboin CO, Griffen AL, Leys EJ (2009) *Porphyromonas gingivalis* strain diversity. J Clin Microbiol **47**, 3073–3081.

[38] Kanagasingam S, Chukkapalli SS, Welbury R, Singhrao SK (2020) *Porphyromonas gingivalis* is a Strong Risk Factor for Alzheimer's Disease. *J Alzheimer's Dis Reports* **4**, 501–511.

[39] Hamamoto Y, Ouhara K, Munenaga S, Shoji M, Ozawa T, Hisatsune J, Kado I, Kajiya M, Matsuda S, Kawai T, Mizuno N, Fujita T, Hirata S, Tanimoto K, Nakayama K, Kishi H, Sugiyama E, Kurihara H (2020) Effect of *Porphyromonas*

gingivalis infection on gut dysbiosis and resultant arthritis exacerbation in mouse model. *Arthritis Res Ther* **22**, 1–15.

[40] Hajishengallis G, Lamont RJ Breaking bad: Manipulation of the host response by *Porphyromonas gingivalis*. *Eur J Immunol* **44**,328-38.

[41] Dhotre S V., Davane MS, Nagoba BS (2017) Periodontitis, bacteremia and infective endocarditis: A review study. *Arch Pediatr Infect Dis* **5**.

[42] Nie R, Wu Z, Ni J, Zeng F, Yu W, Zhang Y, Kadowaki T, Kashiwazaki H, Teeling JL, Zhou Y (2019) *Porphyromonas gingivalis* Infection Induces Amyloid-β Accumulation in Monocytes/Macrophages. *J Alzheimer's Dis* 1–16.

[43] Ilievski V, Zuchowska PK, Green SJ, Toth PT, Ragozzino ME, Le K, Aljewari HW, O'Brien-Simpson NM, Reynolds EC, Watanabe K (2018) Chronic oral application of a periodontal pathogen results in brain inflammation, neurodegeneration and amyloid beta production in wild type mice. *PLoS One* **13**.

[44] Wang T, Lafuse WP, Zwilling BS (2001) NFκB and Sp1 Elements Are Necessary for Maximal Transcription of Toll-like Receptor 2 Induced by Mycobacterium avium. *J Immunol* **167**, 6924–6932.

[45] Boaru SG, Borkham-Kamphorst E, Van De Leur E, Lehnen E, Liedtke C, Weiskirchen R (2015) NLRP3 inflammasome expression is driven by NF-κB in cultured hepatocytes. *Biochem Biophys Res Commun* **458**, 700–706.

[46] Liu T, Zhang L, Joo D, Sun SC (2017) NF-κB signaling in inflammation. *Signal Transduct Target Ther* **2**, 1–9.

[47] Lee DJ, Du F, Chen SW, Nakasaki M, Rana I, Shih VFS, Hoffmann A, Jamora C

(2015) Regulation and Function of the Caspase-1 in an Inflammatory Microenvironment. *J Invest Dermatol* **135**, 2012–2020.

[48] Minger SL, Honer WG, Esiri MM, Mcdonald B, Keene J, Nicoll JAR, Carter J, Hope T, Francis PT (2001) Synaptic pathology in prefrontal cortex is present only with severe dementia in Alzheimer disease. *J Neuropathol Exp Neurol* **60**, 929–936.

[49] Fremeau RT, Voglmaier S, Seal RP, Edwards RH (2004) VGLUTs define subsets of excitatory neurons and suggest novel roles for glutamate. *Trends Neurosci* **27**, 98–103.

[50] Mertens R, Melchert S, Gitler D, Schou MB, Saether SG, Vaaler A, Piepgras J, Kochova E, Benfenati F, Ahnert-Hilger G, Ruprecht K, Höltje M (2018) Epitope specificity of anti-synapsin autoantibodies: Differential targeting of synapsin I domains. *PLoS One* **13**, e0208636.

[51] Rosi S (2011) Neuroinflammation and the plasticity-related immediate-early gene Arc. *Brain Behav Immun* **25**.

FIGURE LEGENDS

Fig.1. The expression of IL-1β and SYP in middle-aged mice after systemic *P. gingivalis* infection. A) The immunofluorescent CLMS images of brain slice stained with SYP (Green) and DAPI (Blue) after systemic *P. gingivalis* infection. (n = 3 mice, each). Scale bar = 25 μm. B) The quantitative analysis of SYP fluorescence density in (A). Asterisks indicate a statistically significant difference from the control group (***p

< 0.001, *t*-test). C) The immunofluorescent CLMS images of brain slice stained with IL-1β (Green), Fibronectin (Red) and DAPI (Blue) after systemic *P. gingivalis* infection. (n = 3 mice, each). Scale bar = 25 μm. D) The quantitative analysis of IL-1β fluorescence density in fibronectin^{+} cells in (C). Asterisks indicate a statistically significant difference from the con group (***$p < 0.001$, *t*-test). ***E***, Pearson's correlation between the IL-1β in (D) and SYP in (B).

Fig. 2. NLRP3 inflammasome activation in *P. gingivalis*-infected leptomeningeal cells. A) The relative cell viability in *P. gingivalis* infected leptomeningeal cells with different MOIs and time points. Each column and bar represent the mean ± SEM (n = 3, each). B) The secretion of IL-1β from leptomeningeal cells after infection with *P. gingivalis* for 1, 3, 6, and 12 h. Each column and bar represent the mean ± SEM (n = 3, each). Asterisks indicate a statistically significant difference from the control group (***$p <$ 0.001, **$p < 0.01$, *t*-test). C) The relative mRNA expression of NLRP3 in leptomeningeal cells after *P. gingivalis* infection with MOI = 10 for 1, 3, 6, and 12 h. Each column and bar represent the mean ± SEM (n = 3, each). Asterisks indicate a statistically significant difference from the control group (***$p < 0.001$, *t*-test). D) Relative mRNA expression of NLRP3 in leptomeningeal cells with *P. gingivalis* infection for 3 h in the presence or absence of NLRP3 siRNA. Each column and bar represent the mean ± SEM (n = 3, each). Asterisks indicate a statistically significant difference between the two groups (***$p < 0.001$, **$p < 0.01$, *t*-test). E) The immunoblots show the pro- and mature-type of caspase-1 in leptomeningeal cells after

infection with *P. gingivalis* for 3 h in the presence or absence of NLRP3 siRNA. F) The quantitative analyses of the mature caspase-1 in (E). Each column and bar represent the mean ± SEM (n = 3, each). Asterisks indicate a statistically significant difference from the control group (***$p < 0.001$, *t*-test). Daggers indicate a statistically significant difference from the *P. gingivalis* infection group. (††$p < 0.01$, *t*-test). G) The immunoblots show the pro- and mature-type of IL-1β in leptomeningeal cells after infection with *P. gingivalis* for 3 h in the presence or absence of NLRP3 siRNA. H) The quantitative analyses of the mature IL-1β in (G). Each column and bar represent the mean ± SEM (n = 3, each). Asterisks indicate a statistically significant difference from the control group (***$p < 0.001$, *t*-test). Daggers indicate a statistically significant difference from the *P. gingivalis* infection group. (††$p < 0.01$, *t*-test). I) IL-1β released from leptomeningeal cells after infection with *P. gingivalis* for 3 h in the presence or absence of NLRP3 siRNA. Each column and bar represent the mean ± SEM (n = 3, each). Asterisks indicate a statistically significant difference from the control group (***$p < 0.001$, *t*-test). Daggers indicate a significant difference from the *P. gingivalis* infection group. (††$p < 0.01$, *t*-test).

Fig. 3. Involvement of CatB in NLRP3 inflammasome activation in *P. gingivalis*-infected leptomeningeal cells. A) CLMS images of *P. gingivalis* infected leptomeningeal cells for 1 h. *P. gingivalis* was labeled with FITC (Green), endosome/lysosome was labeled with LAMP2 (Red) and cell nucleus was labeled with DAPI (Blue). Scale bar = 20 μm. B) CLMS images of acridine orange in control and *P.*

gingivalis infected leptomeningeal cells for 2 h. Scale bar = 20 μm. C) The immunoblots show the CatB in the cytosol of leptomeningeal cells after infection with *P. gingivalis* for 2 h. D) The quantitative analyses of the immunoblot in (C). Each column and bar represent the mean ± SEM (n = 3, each). Asterisks indicate a statistically significant difference from the control group (**$p < 0.01$, *t*-test). E) The immunoblots show the pro- and mature-type of caspase-1 in leptomeningeal cells after infection with *P. gingivalis* for 3 h in the presence or absence of 10 μM CA-074Me. F) The quantitative analyses of the mature caspase-1 in (E). Each column and bar represent the mean ± SEM (n = 3, each). Asterisks indicate a statistically significant difference from the control group (***$p < 0.001$, *t*-test). Daggers indicate a statistically significant difference from the *P. gingivalis* infection group (†††$p < 0.001$, *t*-test). G) The IL-1β released from leptomeningeal cells after infection with *P. gingivalis* for 3 h in the presence or absence of CA-074Me. Each column and bar represent the mean ± SEM (n = 3, each). Asterisks indicate a statistically significant difference from the control group (***$p < 0.001$, *t*-test). Daggers indicate a significant difference from the *P. gingivalis* infection group (††$p < 0.01$, *t*-test). H) The immunoblots show the pro- and mature-type of IL-1β in leptomeningeal cells after infection with *P. gingivalis* for 3 h with or without 1 μM CytoD. I) The quantitative analyses of the mature IL-1β in (H). Each column and bar represent the mean ± SEM (n = 3, each). Asterisks indicate a statistically significant difference from the control group (***$p < 0.001$, *t*-test). Daggers indicate a statistically significant difference from the *P. gingivalis* infection group (††$p < 0.01$, *t*-test). J) The secretion of IL-1β from leptomeningeal cells after infection with *P.*

gingivalis for 3 h with or without Cyto D. Each column and bar represent the mean ± SEM (n = 3, each). Asterisks indicate a statistically significant difference from the control group (***$p < 0.001$, *t*-test). Daggers indicate a statistically significant difference from the *P. gingivalis* infection group (†††$p < 0.001$, *t*-test).

Fig. 4. Involvement of CatB in the activation of NF-κB in *P. gingivalis*-infected leptomeningeal cells. A) The immunoblots show the CatB in leptomeningeal cells after infection with *P. gingivalis* for 0.5, 1, 2, and 3 h. B) The quantitative analyses of CatB in the immunoblot shown in (A). Each column and bar represent the mean ± SEM (n = 3, each). Asterisks indicate a statistically significant difference from the control group (***$p < 0.001$, **$p < 0.01$, *$p < 0.05$, *t*-test). C) The immunoblots show the IκBα in leptomeningeal cells after infection with *P. gingivalis* for 1 h with or without pretreatment with 10 μM CA-074Me. D) The quantitative analyses of total IκBα in the immunoblot shown in (C). Each column and bar represent the mean ± SEM (n = 3, each). Asterisks indicate a statistically significant difference from the control group (**$P < 0.01$, *t*-test). A dagger indicates a significant difference from the *P. gingivalis* infection group. (†$p < 0.05$, *t*-test). E), F), G) Relative mRNA expression of NLRP3 (E), Caspase-1 (F), and IL-1β (G) in leptomeningeal cells after *P. gingivalis* infection with or without CA-074Me pretreatment. Each column and bar represent the mean ± SEM (n = 3, each). Asterisks indicate a statistically significant difference from the control group (***$p < 0.001$, *t*-test). Daggers indicate a statistically significant difference from the *P. gingivalis* infection group (†††$p < 0.001$, *t*-test). H) The

immunoblots show the pro- and mature-type of IL-1β in leptomeningeal cells after infection with *P. gingivalis* for 3 h in the presence or absence of CA-074Me. I), J) The quantitative analyses of the immunoblots in (H). Each column and bar represent the mean ± SEM (n = 3, each). Asterisks indicate a statistically significant difference from the control group (***$p < 0.001$, *t*-test). Daggers indicate a statistically significant difference from the *P. gingivalis* infection group (†††$p < 0.001$, †$p < 0.05$, *t*-test).

Fig. 5. Involvement of *P. gingivalis*-infected leptomeningeal cells in synaptic molecules in neurons. Condition medium from leptomeningeal cells infected by *P. gingivalis* for 3 h with MOI=10 (*Pg* LCM). A) The relative cell viability in control and *Pg* LCM neurons. Each column and bar represent the mean ± SEM (n = 3, each). B) CLMS images of primary neurons (MAP2, red) with or without *Pg* LCM treatment. C) The neurite length analyses of the neurons in (B). Each column and bar represent the mean ± SEM (n = 10, each). Asterisks indicate a statistically significant difference from the control group (**$p < 0.01$, *t*-test). D) The relative mRNA expression of SYP, VGLUT1, and SYN1 in control and *Pg* LCM neurons. Each column and bar represent the mean ± SEM (n = 3, each). Asterisks indicate a statistically significant difference from the control group (***$p < 0.001$, *t*-test). E) Pearson's correlation between the secreted IL-1β in *Pg* LCM and synaptic components in (D). F) The immunoblots show SYP in control, *Pg* LCM, *Pg*+NLRP3kd LCM, and *Pg*+CA LCM incubated primary neurons. G) Quantitative analyses of the immunoblots in (F). Each column and bar represent the mean ± SEM (n = 3, each). Asterisks indicate a statistically significant difference from

the control group (***p < 0.001, t-test). Daggers indicate a statistically significant difference from the *Pg* LCM group. (†††p < 0.001, †p < 0.05, t-test). H) The immunoblots show SYP in primary neurons with or without 1 μg/ml IL-1Ra pretreatment followed by incubation with *Pg* LCM. I) Quantitative analyses of the immunoblots in (H). Each column and bar represent the mean ± SEM (n = 3, each). Asterisks indicate a statistically significant difference from the control group (***p < 0.001, t-test). Daggers indicate a statistically significant difference from the *Pg* LCM group. (†††p < 0.001, t-test).

Fig.6. Involvement of *P. gingivalis*-infected leptomeningeal cells in BDNF/CREB signaling in neurons. A) CLMS images of p-CREB after treatment with *Pg* LCM, BDNF and IL-1Ra. Scale bar = 10 μm. B) The quantitative analysis of relative p-CREB fluorescent in (A). Each column and bar represent the mean ± SEM (n = 10, each). Asterisks indicate a statistically significant difference between indicated groups (***p < 0.001, **p < 0.01, *p < 0.1, t-test). C) The expression of p-CREB and total CREB protein after treatment with *Pg* LCM, BDNF, and IL-1Ra. D) The quantitative analyses of p-CREB/CREB in the immunoblot shown in (C). Each column and bar represent the mean ± SEM (n = 3, each). Asterisks indicate a statistically significant difference (**p < 0.01, *p < 0.05, t-test).

Fig. 7. A schematic representation showing the effects of leptomeningeal cells in inducting synaptic failure after *P. gingivalis* infection. In leptomeningeal cells, *P.*

gingivalis induces activation of NF-κB for production of pro IL-1β, NLRP3, pro-caspase-1 and CatB. CatB degrades IκBα to prolong activation of NF-κB during binding to its receptors. At the same time, the phagocytized *P. gingivalis* into the lysosome induces lysosomal rupture resulting in CatB leakage into cytosol. The cytosol CatB activates NLRP3 inflammasome (capase-1) thus resulting in the maturation and secretion of IL-1β. In neurons, the leptomeningeal cell-produced IL-1β suppresses BDNF/CREB signaling resulting in decrease of synaptic molecules, including SYP, SYN1 and VGLUT1.

Figure. 1

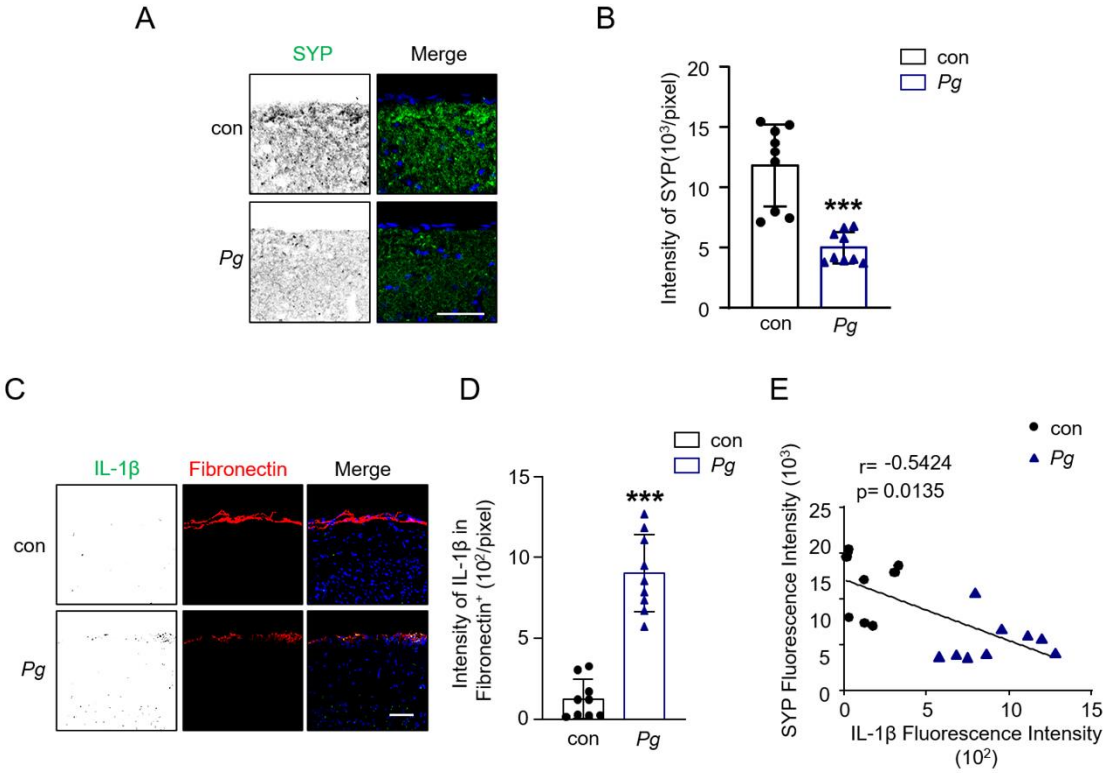
A
SYP
Merge
con
Pg
B
con
Pg
Intensity of SYP(10³/pixel)
20
15
10
5
0
***
con
Pg
C
IL-1β
Fibronectin
Merge
con
Pg
D
con
Pg
Intensity of IL-1β in Fibronectin⁺ (10²/pixel)
15
10
5
0
***
con
Pg
E
con
Pg
r= -0.5424
p= 0.0135
SYP Fluorescence Intensity (10³)
25
20
15
10
5
0
0
5
10
15
IL-1β Fluorescence Intensity (10²)

Figure. 2

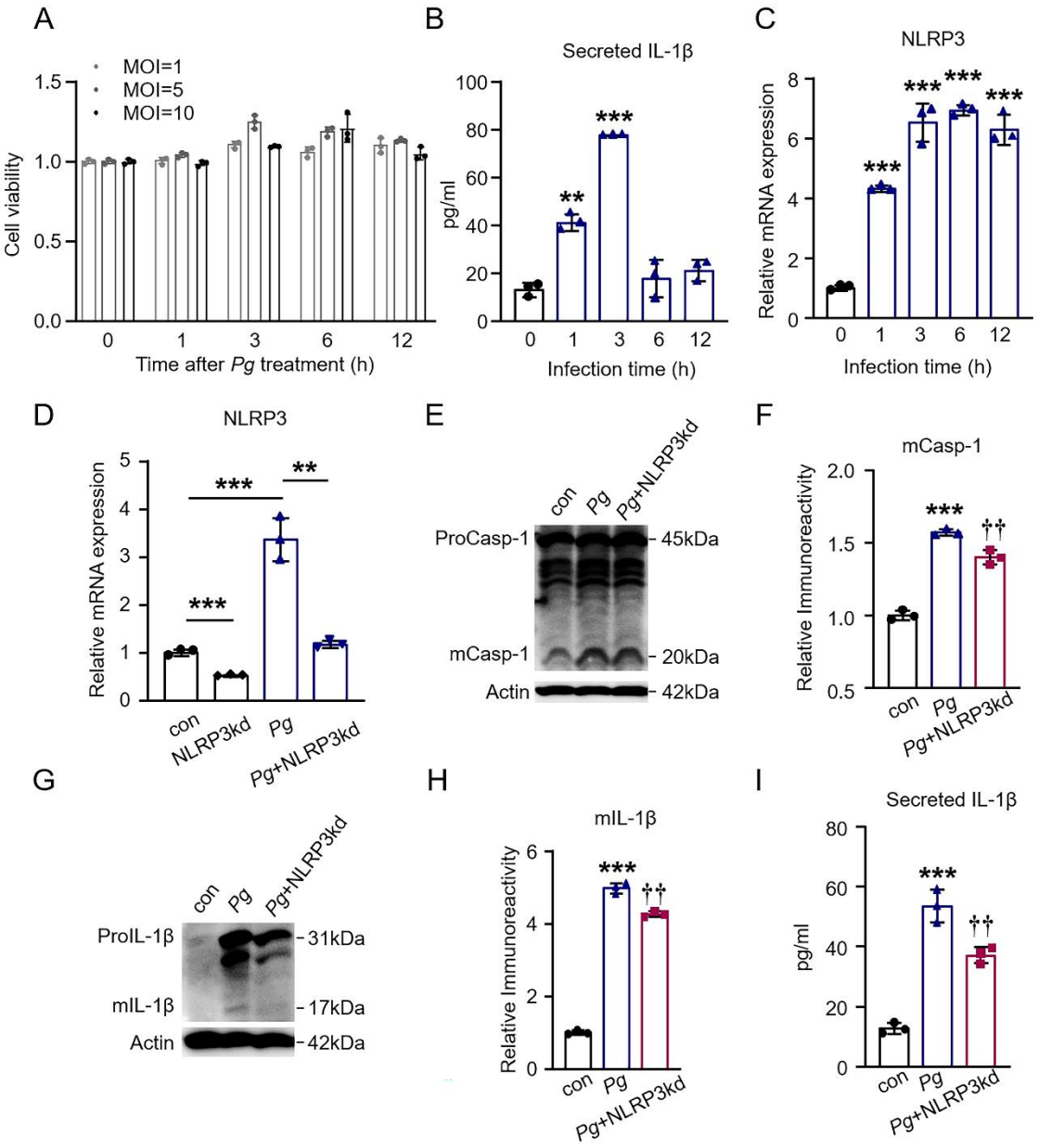
A
MOI=1
MOI=5
MOI=10
Cell viability
Time after Pg treatment (h)
B
Secreted IL-1β
pg/ml
Infection time (h)
C
NLRP3
Relative mRNA expression
Infection time (h)
D
NLRP3
Relative mRNA expression
con
NLRP3kd
Pg
Pg+NLRP3kd
E
con
Pg
Pg+NLRP3kd
ProCasp-1
45kDa
mCasp-1
20kDa
Actin
42kDa
F
mCasp-1
Relative Immunoreactivity
G
ProIL-1β
31kDa
mIL-1β
17kDa
Actin
42kDa
H
mIL-1β
Relative Immunoreactivity
I
Secreted IL-1β
pg/ml

Figure. 3

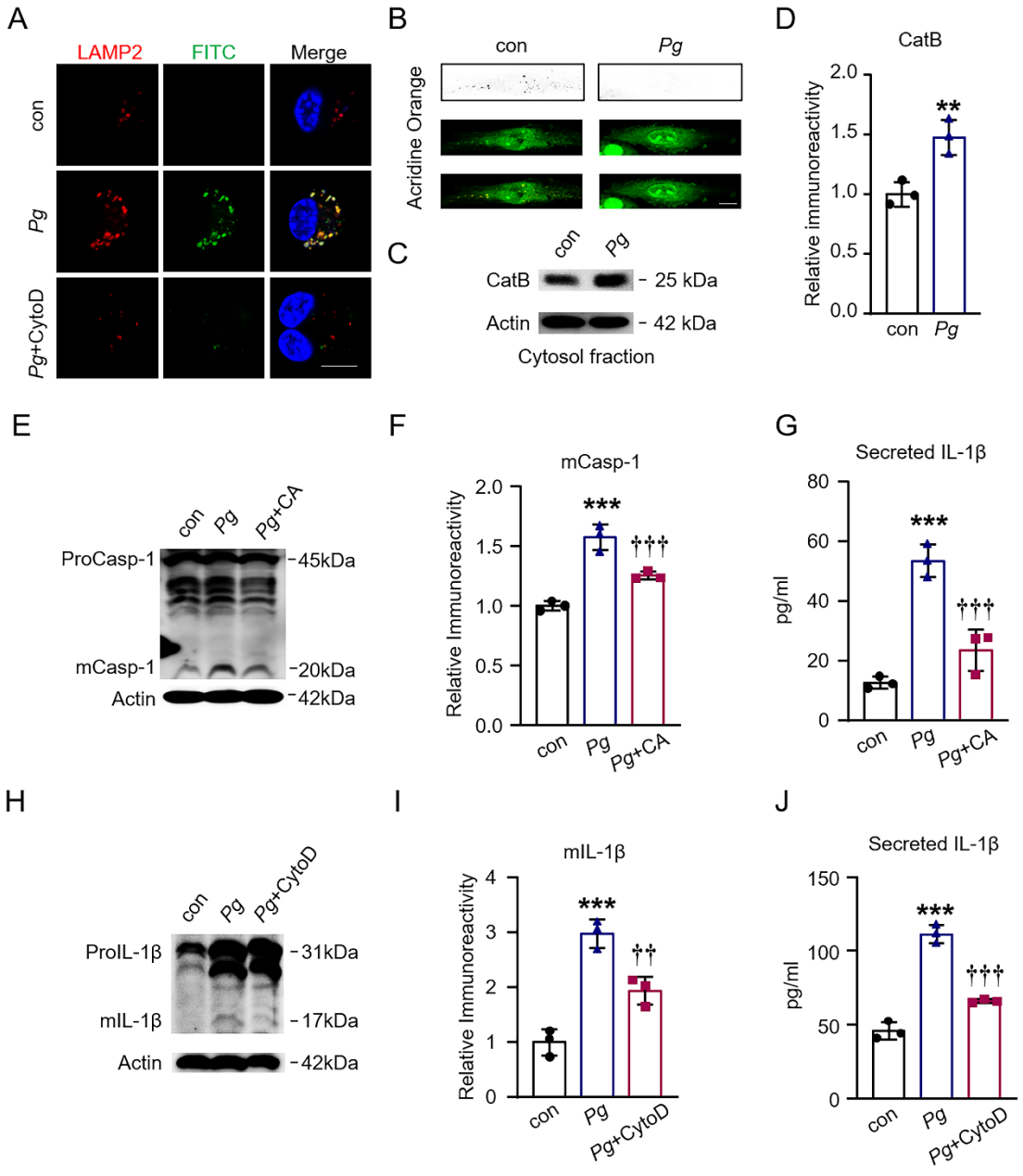
A
LAMP2
FITC
Merge
con
Pg
Pg+CytoD
B
con
Pg
Acridine Orange
C
con
Pg
CatB
25 kDa
Actin
42 kDa
Cytosol fraction
D
CatB
Relative immunoreactivity
2.0
1.5
1.0
0.5
0.0
**
con
Pg
E
con
Pg
Pg+CA
ProCasp-1
45kDa
mCasp-1
20kDa
Actin
42kDa
F
mCasp-1
Relative Immunoreactivity
2.0
1.5
1.0
0.5
0.0
***
†††
con
Pg
Pg+CA
G
Secreted IL-1β
pg/ml
80
60
40
20
0
***
†††
con
Pg
Pg+CA
H
con
Pg
Pg+CytoD
ProIL-1β
31kDa
mIL-1β
17kDa
Actin
42kDa
I
mIL-1β
Relative Immunoreactivity
4
3
2
1
0
***
††
con
Pg
Pg+CytoD
J
Secreted IL-1β
pg/ml
150
100
50
0
***
†††
con
Pg
Pg+CytoD

Figure. 4

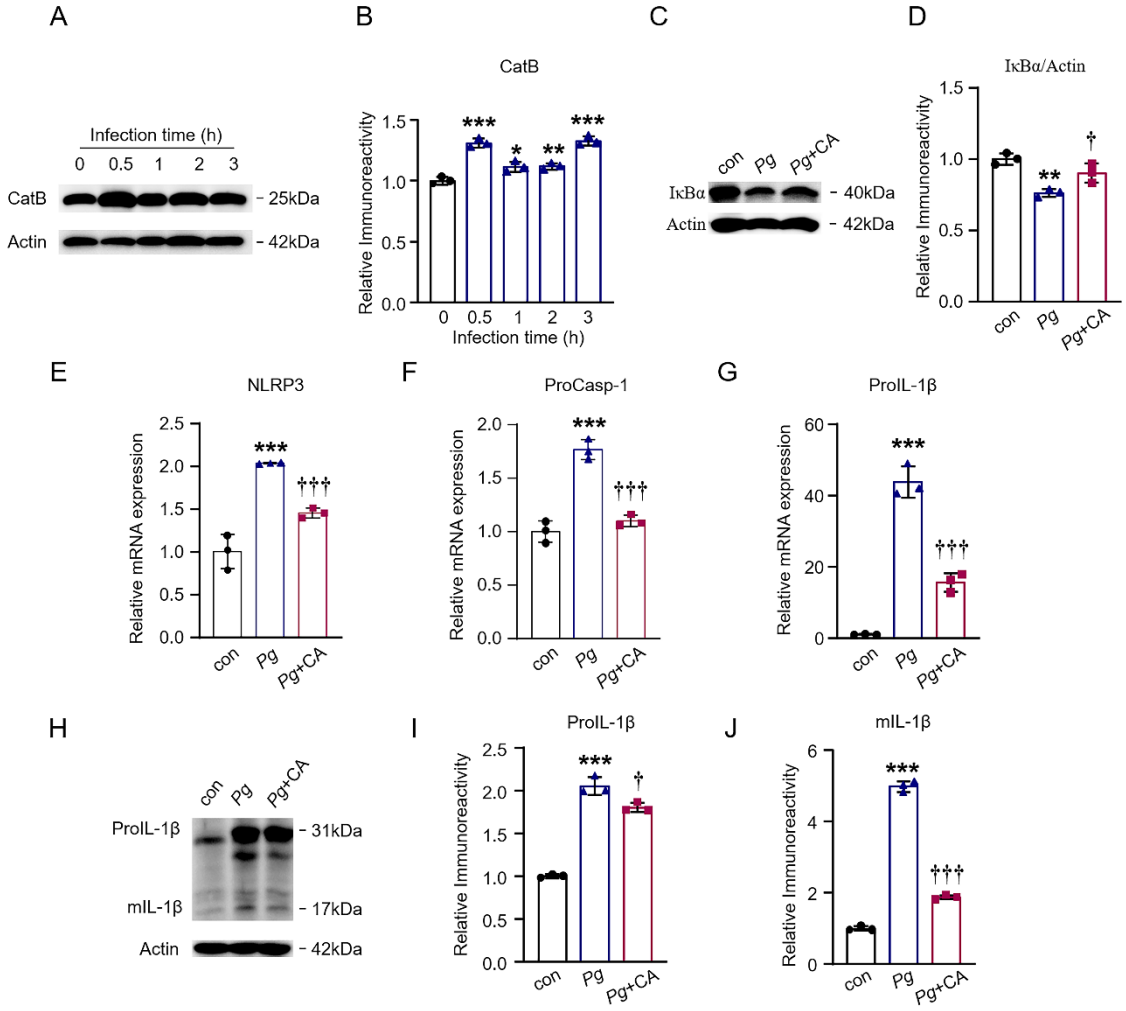
A
Infection time (h)
0 0.5 1 2 3
CatB
- 25kDa
Actin
- 42kDa
B
CatB
Relative Immunoreactivity
Infection time (h)
C
con Pg Pg+CA
IκBα
- 40kDa
Actin
- 42kDa
D
IκBα/Actin
Relative Immunoreactivity
E
NLRP3
Relative mRNA expression
F
ProCasp-1
Relative mRNA expression
G
ProIL-1β
Relative mRNA expression
H
con Pg Pg+CA
ProIL-1β
- 31kDa
mIL-1β
- 17kDa
Actin
- 42kDa
I
ProIL-1β
Relative Immunoreactivity
J
mIL-1β
Relative Immunoreactivity

Figure. 5

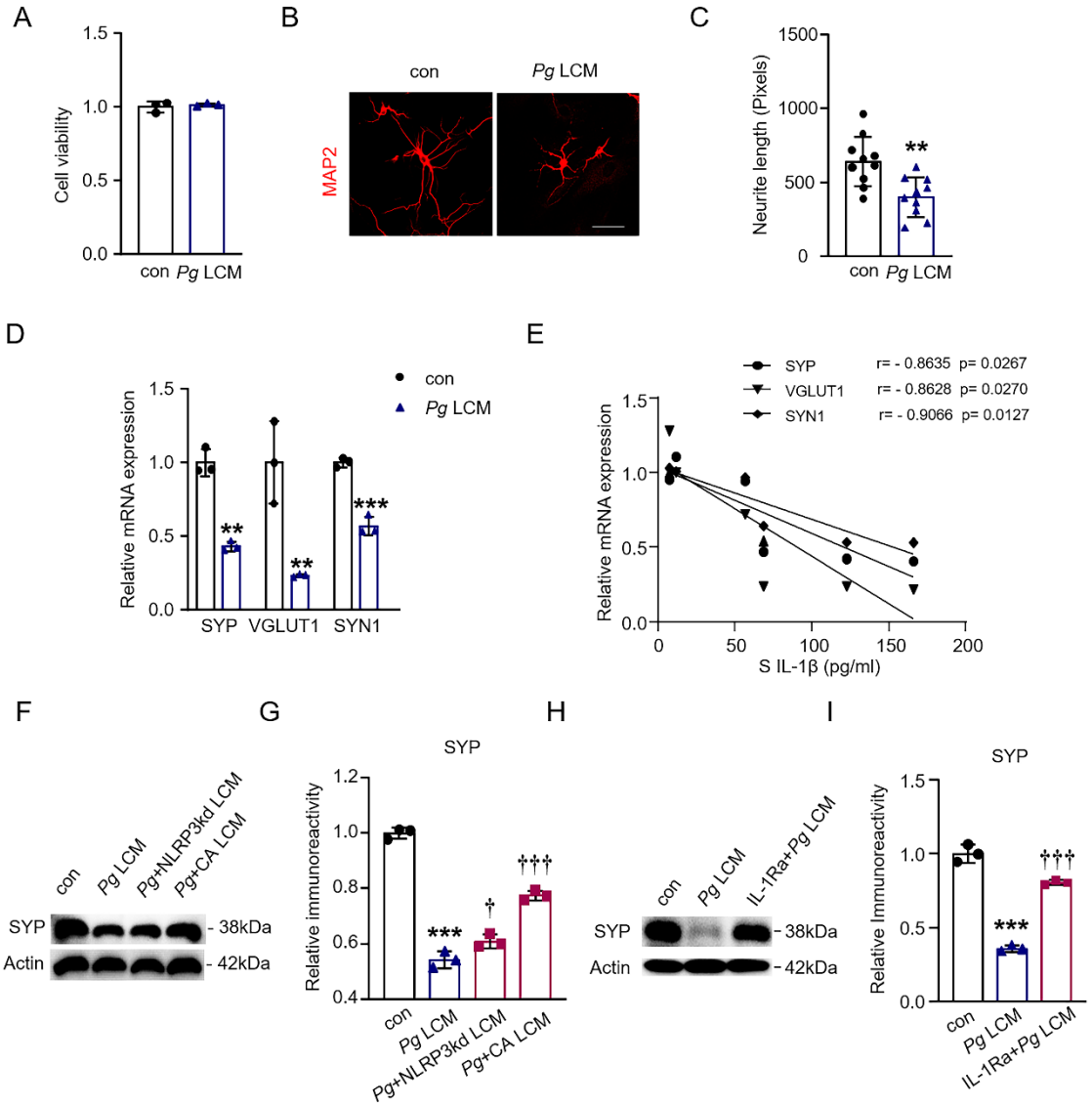
A
Cell viability
1.5
1.0
0.5
0.0
con Pg LCM
B
con
Pg LCM
MAP2
C
Neurite length (Pixels)
1500
1000
500
0
**
con Pg LCM
D
con
Pg LCM
Relative mRNA expression
1.5
1.0
0.5
0.0
**
**
***
SYP VGLUT1 SYN1
E
SYP r= - 0.8635 p= 0.0267
VGLUT1 r= - 0.8628 p= 0.0270
SYN1 r= - 0.9066 p= 0.0127
Relative mRNA expression
1.5
1.0
0.5
0.0
0 50 100 150 200
S IL-1β (pg/ml)
F
con
Pg LCM
Pg+NLRP3kd LCM
Pg+CA LCM
SYP
- 38kDa
Actin
- 42kDa
G
SYP
Relative immunoreactivity
1.2
1.0
0.8
0.6
0.4
***
†
†††
con
Pg LCM
Pg+NLRP3kd LCM
Pg+CA LCM
H
con
Pg LCM
IL-1Ra+Pg LCM
SYP
- 38kDa
Actin
- 42kDa
I
SYP
Relative Immunoreactivity
1.5
1.0
0.5
0.0
***
†††
con
Pg LCM
IL-1Ra+Pg LCM

Figure. 6

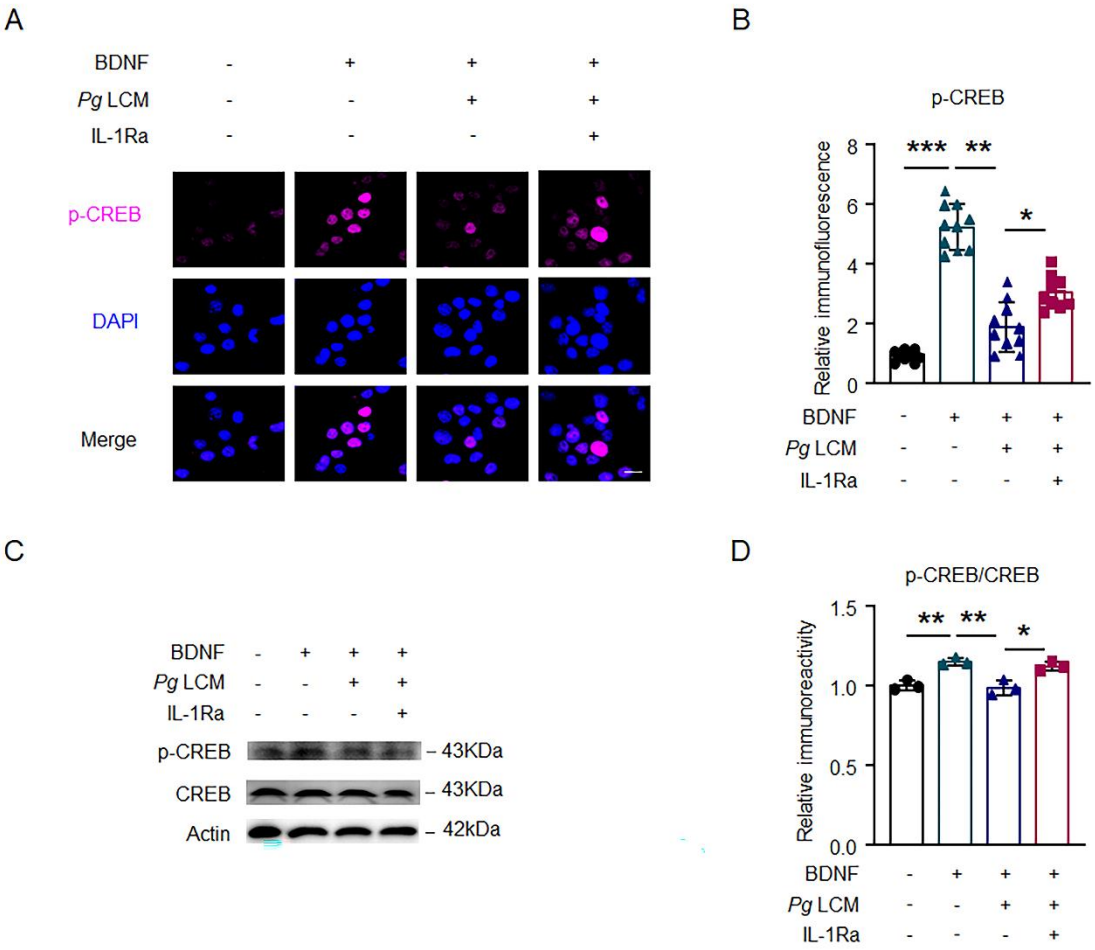
A
BDNF - + + +
Pg LCM - - + +
IL-1Ra - - - +
p-CREB
DAPI
Merge
B
p-CREB
Relative immunofluorescence
0 2 4 6 8
*** **
*
BDNF - + + +
Pg LCM - - + +
IL-1Ra - - - +
C
BDNF - + + +
Pg LCM - - + +
IL-1Ra - - - +
p-CREB – 43KDa
CREB – 43KDa
Actin – 42kDa
D
p-CREB/CREB
Relative immunoreactivity
0.0 0.5 1.0 1.5
** **
*
BDNF - + + +
Pg LCM - - + +
IL-1Ra - - - +

Figure. 7

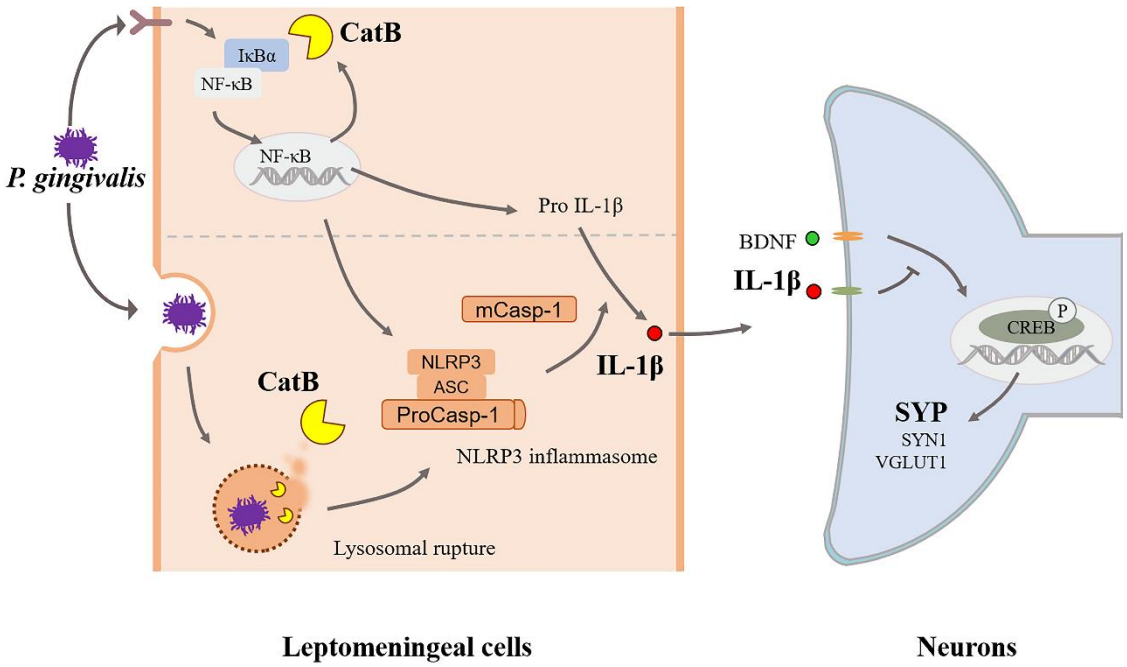
CatB
IκBα
NF-κB
NF-κB
P. gingivalis
Pro IL-1β
mCasp-1
NLRP3
ASC
ProCasp-1
IL-1β
CatB
NLRP3 inflammasome
Lysosomal rupture
BDNF
IL-1β
P
CREB
SYP
SYN1
VGLUT1
Leptomeningeal cells
Neurons